

A Theory of Resistive Hose Instability in Intense Charged Particle Beams Propagating Through Background Plasma With Low Electron Collision-Frequency

Han S. Uhm, *Senior Member, IEEE*, and Ronald C. Davidson

Abstract—Stability properties of the resistive hose instability is investigated for a rounded current-density profile of a charged particle beam propagating through a background plasma where the electron collision time ($1/\nu_c$) is comparable to or longer than the magnetic decay time (τ_d). The eigenvalue equation is derived based on the energy group model, including the stabilizing influence of a finite magnetic decay time. The dispersion relation of the resistive hose instability in a charged particle beam with an arbitrary current density profile is derived, assuming that the eigenfunctions can be represented by the rigid displacement of the self magnetic field in the plasma. Stability analysis for perturbations propagating through the beam pulse from its head to tail is carried out for an arbitrary current profile of the beam. It is shown from the stability analysis that the width of the range Ω^2 corresponding to instability decreases drastically as the value of parameter $\nu_c\tau_d$ decreases from infinity to zero, thereby being a very narrow bandwidth of instability. It is also shown for arbitrary current profile that any perturbation with frequency Ω higher than the maximum betatron frequency $\omega_{\beta m}$ is stable. Here, Ω is the Doppler-shifted frequency seen by beam particles.

Index Terms—Beam instability, beam propagation, charged particle beam, resistive hose.

I. INTRODUCTION

THERE is a growing interest on intense charged particle beams [1]–[5] due to a wide range of applications, including basic scientific research, spallation neutron source, nuclear waste transmutation, and heavy ion fusion [6]–[8]. Background electrons and plasmas are often present at the high ion current densities of practical interest. It has been recognized [9]–[19] for many years that the relative streaming motion of a charged particle beam through a background charge species provides a free energy to drive the classical two-stream instability. In addition, the presenting background plasma may act like a resistive medium, which may drive the resistive hose instability [20]–[27] in the propagating ion beam. When a current-carrying beam moves through conducting plasma, its self-magnetic field may follow the beam with a delay time called the magnetic decay time τ_d . The magnetic

field lines are frozen into the plasma, pulling back the distorted beam segment if the plasma is highly conducting. However, this restoring mechanism, which leads to the resistive hose instability, overshoots and grows due to the motionless resistive plasma medium [21]–[27], where the electron collision time ($1/\nu_c$) is much shorter than the magnetic decay time (τ_d). The electron collision frequency ν_c for an electron temperature $T_e \approx 1$ eV is about 10^{11} s^{-1} in ambient air at one atmospheric pressure leading to $\nu_c\tau_d \gg \gg 1$, where the electron collisions are dominated by electron-neutral collisions.

Obviously, the electron collision frequency decreases considerably if plasma channel is preformed in a low-pressure chamber. For example, consider an ion beam propagating through a preformed plasma channel. Assuming plasma electron temperature $T_e = 1$ eV and electron density $n_e = 5 \times 10^{12} \text{ cm}^{-3}$, the electron collision frequency due to Coulomb collisions is $\nu_c = 1.5 \times 10^8 \text{ s}^{-1}$. The magnetic decay time is calculated to be $\tau_d = 9 \times 10^{-10} \text{ s}$, leading to $\nu_c\tau_d = 0.135$, which is much less than unity. If the plasma electron collision time ($1/\nu_c$) is comparable to or longer than the magnetic decay time τ_d , some of the magnetic field lines may slip through the plasma following the beam's transverse motion, thereby weakening the instability mechanism of the resistive hose instability. A recent literature [28] investigated effects of the electron collisions on the resistive hose instability in charged particle beams with a flattop density profile. However, the instability growth rate for the flattop density profile is unrealistically infinite at the resonance frequency due to the same betatron frequency of all the charged particles in the flattop density. Most of the charged particle beams have a rounded density profile. Therefore, there is no one-resonance frequency for all the beam particles to execute. In this context, stability properties of the resistive hose instability are investigated for a rounded current-density profile of a charged particle beam propagating through a background plasma where the electron collision time ($1/\nu_c$) is comparable to or longer than the magnetic decay time (τ_d). For applications to intense ion beams for heavy ion beam fusion [29]–[32], both assisted-pinch transport [29], [30] in the target chamber and neutralized ballistic transport [31], [32] through background plasma are possible modes for beam propagation. The present analysis is most applicable to assisted-pinch transport since the beam radius is assumed to be approximately constant.

The basic assumptions and theoretical model are presented in Section II, where a charged particle beam with a rounded density

Manuscript received February 23, 2005; revised April 15, 2005. This work was supported by the U.S. Department of Energy.

H. S. Uhm is with the Department of Molecular Science and Technology, Ajou University, Suwon 443-749, Korea.

R. C. Davidson is with the Plasma Physics Laboratory, Princeton University, Princeton, NJ 08543 USA.

Digital Object Identifier 10.1109/TPS.2005.853028

profile propagates through a background plasma channel. The electron collision time ($1/\nu_c$) in the plasma channel is assumed to be comparable to the magnetic decay time (τ_d) of the plasma. The eigenvalue equation is derived in Section II based on the energy group model [23], assuming long-wavelength, low-frequency perturbations and the complete charge neutralization [33] of the perturbed beam space-charge field. The eigenvalue equation obtained in Section II includes the stabilizing influence of a finite magnetic decay time, which can be comparable to or shorter than the electron collision time ($1/\nu_c$).

The dispersion relation of the resistive hose instability in a charged particle beam with an arbitrary current density profile is derived in Section III, assuming that the eigenfunctions can be represented by the rigid displacement of the self magnetic field in the plasma, which is a reasonable approximation for low-frequency perturbations. The perturbations are Fourier decomposed according to $\exp[-i(\omega\tau + \Omega z/\beta_b c)]$, where $\tau = t - z/\beta_b c$ represents the coordinate measured from the head of the beam to the tail, and Ω is the Doppler-shifted frequency seen by a beam particle. Here, $\beta_b c$ is the average axial beam velocity, and ω are the eigenfrequency of perturbations. The dispersion relation will be analyzed according to the nature of the initial perturbation at the beam head. In other words, the beam segment may be treated by using z and τ as independent variables. Stability analysis for perturbations propagating through the beam pulse from its head to tail is carried out in Section III for an arbitrary current profile of the beam, by selecting z and τ as independent variables. In this case, the Doppler-shifted frequency Ω seen by the beam particles scales as the characteristic transverse betatron frequency $\omega_{\beta m}$ of the beam particles. In addition, the frequency ω scales as the magnetic decay time in the plasma channel. The complex eigenfrequency ω in the dispersion relation of the resistive hose instability in a beam with an arbitrary current profile is expressed as a function of the real oscillation frequency Ω of each beam segment. Then, the imaginary value of the eigenfrequency ω determines the growth of the perturbation as one moves backward from the head of the beam. It is shown from the stability analysis in Section III that the width of the range Ω^2 corresponding to instability decreases drastically as the value of parameter $\nu_c \tau_d$ decreases from infinity to zero and the fractional current neutralization f approaches unity, thereby being a very narrow bandwidth of instability. Thus, the instability caused by the dynamics of the beam segments with frequency Ω may easily be avoided by choosing proper system parameters for a finite value of parameter $\nu_c \tau_d$, which can be much less than unity in some practical applications. The parameter $\nu_c \tau_d$ less than unity means that the electron collision time ($1/\nu_c$) is longer than the magnetic decay time (τ_d). It is also shown for arbitrary current profile that any perturbation with frequency Ω higher than the maximum betatron frequency $\omega_{\beta m}$ is stable (purely damping). Stability properties of the resistive hose instability in a beam with Bennett current profile are investigated in Section IV as an example of the rounded beam density. Stability properties analyzed numerically in Section IV for the Bennett current profile agree well with the general discussions in Section III for an arbitrary current profile.

II. BASIC ASSUMPTIONS AND THEORETICAL MODEL

We assume that an intense charged particle beam with radius r_b propagates through background plasma. The conductivity is determined primarily by the plasma electrons. The beam-plasma system is confined transversely within a perfectly conducting cylindrical wall with radius r_w . Cylindrical polar coordinates (r, θ, z) are used, with the z -axis along the axis of symmetry. In equilibrium, both the beam and plasma are assumed to be azimuthally symmetric ($\partial/\partial\theta = 0$), infinitely long, and axially uniform ($\partial/\partial z = 0$). The background plasma, whose density is comparable to or higher than the beam density, is assumed to provide complete neutralization [33] of the beam space charge, and the motion of the beam is assumed to be paraxial ($p_z^2 \gg p_r^2 + p_\theta^2$). The beam particles are radially confined by the self-magnetic field produced by the axial current of the beam, thereby implicating a self-pinch particle beam, where the density profile is a monotonously decreasing function of the radial coordinate. Otherwise, some external forces are needed to generate a beam density profile, which may not be a monotonously decreasing function of the radial coordinate. For example, a hollow charged beam can be generated by an axial plasma current in opposite direction, which provides defocusing forces to the beam particles and which is one of the external force beyond the beam. The subsequent analysis is restricted to the self-pinch particle beam.

Under the assumption that the equilibrium distribution function for the beam particles is axisymmetric and spatially uniform in the axial direction, we recognize that the transverse Hamiltonian and axial momentum of the beam particles are constants of the motion in the equilibrium fields [5], [19], [23], [28]. Therefore, for present purposes, the equilibrium distribution function for the beam particles is taken to be [23]

$$F_b^0(H_{\perp b}, p_z) = \frac{n_b}{2\pi\gamma_b m_b} F(H_{\perp b}) G_b(p_z) \quad (1)$$

where $n_b = \text{constant}$ is the number density of the beam particles on axis and m_b is the rest mass of the beam particles. The quantity $H_{\perp b}$ occurring in (1) is the transverse Hamiltonian defined by

$$H_{\perp b} = \frac{1}{2\gamma_b m_b} p_{\perp}^2 + \Psi_0(r) \quad (2)$$

where $\Psi_0(r)$ is defined by $\Psi_0(r) = Z_b e \beta_b A_0(r)$, $Z_b e$ is the charge of a beam particle, $\beta_b c$ is the mean axial velocity of the beam particles defined by $\beta_b = (\gamma_b^2 - 1)^{1/2}/\gamma_b$, c is the speed of light in *vacuo*, and $A_0(r)$ is the axial component of the equilibrium vector potential. In (2), $r = (x^2 + y^2)^{1/2}$ is the radial distance from the beam axis, and the axial momentum distribution is normalized according to

$$\int_{-\infty}^{\infty} G_b(p_z) dp_z = 1. \quad (3)$$

Substituting (1) into

$$n_b^0(r) = \int d^3p F_b^0(H_{\perp b}, p_z) \quad (4)$$

we obtain the beam density

$$n_b^0(r) = n_b \int_{\Psi_0(r)}^{\infty} dU F(U) \quad (5)$$

where $U = H_{\perp b}$ is an effective transverse energy variable and the lower limit of integration, $\Psi_0(r)$, is the minimum possible value of $H_{\perp b}$ for a charged particle at r . We note that (5) can be interpreted as representing the beam as a superposition of many groups of beam particles, each characterized by a particular value of transverse energy U

$$n_b^0(r) = \int_0^{\infty} dU F(U) n_0(r; U) \quad (6)$$

where

$$n_0(r; U) = n_b \begin{cases} 1, & r < R(U) \\ 0, & r > R(U) \end{cases} \quad (7)$$

and $R(U)$ is the maximum radius for beam particles of energy U , determined by the condition

$$\Psi_0[R(U)] = U. \quad (8)$$

The axial component $A_0(r)$ of the equilibrium vector potential associated with the self-generated azimuthal field $B_{0\theta}(r)$ is obtained from the Ampere's law

$$-\frac{1}{r} \frac{d}{dr} r \frac{d}{dr} A_0(r) = \frac{1}{r} \frac{d}{dr} r B_{0\theta}(r) = \frac{4\pi}{c} [J_b^0(r) + J_p^0(r)] \quad (9)$$

where $J_b^0(r)$ and $J_p^0(r)$ are the axial beam and plasma-return current densities, respectively. The axial beam-current density $J_b^0(r)$ is related to the beam density $n_b^0(r)$ by $J_b^0(r) = Z_b e \beta_b c n_b^0(r)$. It will be useful to rewrite (5) in the form

$$\begin{aligned} \frac{1}{r} \frac{dn_b^0}{dr} &= -n_b F[\Psi_0(r)] \frac{1}{r} \frac{d\Psi_0(r)}{dr} \\ &= -n_b F[\Psi_0(r)] Z_b e \beta_b \frac{1}{r} \frac{dA_0}{dr} \\ &= \gamma_b m_b n_b F[\Psi_0(r)] \omega_\beta^2(r) \end{aligned} \quad (10)$$

where the betatron frequency $\omega_\beta(r)$ is defined by

$$\begin{aligned} \omega_\beta^2(r) &= Z_b e \beta_b \frac{B_{0\theta}(r)}{\gamma_b m_b r} \\ &= \frac{4\pi Z_b e \beta_b}{\gamma_b m_b c r^2} (1-f) \int_0^r dr' r' J_b^0(r') \end{aligned} \quad (11)$$

and f is the fractional current neutralization caused by the plasma return current, i.e., $J_p^0(r) = -f J_b^0(r)$. The physically acceptable value of f is less than unity. The charged particle density $n_b^0(r)$ is a decreasing function of the radial coordinate r in general. Therefore, we also note from (11) that the betatron frequency for a rounded beam profile is a decreasing function of the radial coordinate r .

The analysis of the resistive hose instability is carried out by making use of the linearized Vlasov–Maxwell equations for the beam equilibria described in (1). We adopt a normal mode approach in which all perturbed quantities are assumed to vary with θ, z , and τ as [23], [28]

$$\psi(\mathbf{x}, t) = \hat{\psi}(r) \exp[i(\theta - \Omega z / \beta_b c - \omega \tau)] \quad (12)$$

where $\tau = t - z / \beta_b c$ is related to the coordinate from the beam head to tail, the Doppler-shifted frequency Ω is the frequency

seen by a beam particle, and ω are the eigenfrequency, respectively. The dispersion relation of the resistive hose instability obtained in the next section relates the eigenfrequency ω to the Doppler-shifted frequency Ω seen by a beam particle. Therefore, the complex eigenfrequency ω is described in terms of the real oscillation frequency Ω of the beam segments. We assume that the plasma is collisional to the extent that it is characterized by a scalar conductivity expressed as

$$\sigma_p(r) = \frac{\sigma(r)}{1 - i\omega / \nu_c} \quad (13)$$

where ν_c is the electron collision frequency. The frequency ω is of the order of the magnetic decay frequency, which is determined by the plasma density. On the other hand, the electron collision frequency ν_c in (13) can be larger or smaller than the frequency ω , depending on the system parameters. The perturbed beam space charge field is assumed to be completely neutralized by the plasma, which requires that [33]

$$4\pi\sigma(r) \gg \omega. \quad (14)$$

We also consider only wavelengths that are long and frequencies that are low compared with quantities that characterize the beam radius r_b , i.e.,

$$\Omega r_b \ll c \quad (15)$$

where c is the speed of light in vacuum. The most-unstable modes satisfy (15), holding the inequality in (14).

It follows that the transverse components of the perturbed fields, B_z, E_r , and E_θ , can be neglected, and that the perturbations can be represented in terms of a perturbed axial component of vector potential Ae_z according to

$$\begin{aligned} B_\theta(r) &= -\frac{dA(r)}{dr} \\ B_r(r) &= \frac{i}{r} A(r) \\ E_z(r) &= -\frac{1}{c} \frac{\partial A(r)}{\partial \tau}. \end{aligned} \quad (16)$$

The plasma electrons respond to the axial component $E_z(r)$ of the perturbed electric field in (16). After carrying out some algebraic manipulations, Ampere's law for the perturbed axial component of vector potential $A(r)$ can be expressed as

$$\frac{d}{dr} \frac{1}{r} \frac{d}{dr} r A(r) + \frac{4\pi i \omega \sigma_p(r)}{c^2} A(r) = -\frac{4\pi}{c} J_b(r) \quad (17)$$

where the conductivity $\sigma_p(r)$ is related to the perturbed axial plasma current $J_p(r)$ by $J_p(r) = \sigma_p E_z(r)$ and the perturbed axial beam current density $J_b(r)$ is calculated from

$$J_b(r) = Z_b e \int d^3 p v_z \delta F_b. \quad (18)$$

The perturbed beam distribution function δF_b occurring in (18) is calculated by the method of the characteristics, which can be expressed as [5], [19], [23], [28]

$$\begin{aligned} \delta F_b(\mathbf{x}, \mathbf{p}, \tau) &= Z_b e G_b(P_z) \frac{\partial}{\partial H_{\perp b}} F_b^0(H_{\perp b}) \\ &\quad \times \int_{-\infty}^{\tau} d\tau' \frac{\mathbf{P}'_{\perp}}{\gamma_b m_b} \cdot \nabla_{\perp} A(\mathbf{x}', \tau') \end{aligned} \quad (19)$$

where use has been made of (15).

For a uniform beam density characterized by $F(H_{\perp b}) = \delta(H_{\perp b} - T_{\perp b})$, the perturbed vector potential is $A(r) \propto r$ and the time integration in (19) can then be carried out [23], [27]. Due to the perturbed surface current density at $r = r_b$ for the uniform beam density, the perturbed vector potential of $A(r) \propto r$ inside the beam is a self-consistent solution. The perturbed beam density $n_{b1}(r)$ for the uniform beam density is calculated to be [23], [28]

$$n_{b1}(r) = \frac{Z_b e \beta_b}{\gamma_b m_b} \frac{A(r)}{\Omega^2 - \omega_\beta^2} n_b \frac{\delta(r - r_b)}{r}. \quad (20)$$

The oscillations of the beam particles in the transverse plane are determined by a ‘‘potential’’ $\Psi_0(r) = Z_b e \beta_b A_0(r)$ in (2) that is anharmonic except for the special case of a beam with uniform density. Beam particles trapped near the axis, i.e., particles with low values of the transverse energy U , oscillate faster than those with large values of U whose orbits reach larger radii. Consequently, a wave with a given real frequency Ω is resonant with some of the beam particles, but not all, and the resonant particles tend to be localized in particular radial ranges of the beam. We have seen from (5)–(8) that the beam is made up of many ‘‘energy groups,’’ i.e., classes of beam particles with a particular narrow range of transverse energy U , and that each energy group has a partial density profile that is flat out to a maximum radius $R(U)$ which is an increasing function of U . We assume that each energy group can be treated as a rigid object, whose center of mass displaces in the transverse plane according to the average magnetic force on all the beam particles in the group. The perturbed current density $J_b(r)$ in (17) can then be written as a sum over the energy groups

$$J_b(r) = Z_b e \beta_b c \int_0^\infty dU F(U) n_1(r; U) \quad (21)$$

where $n_1(r; U)$ is the linearized first-order density corresponding to the rigid displacement of $n_0(r; U)$ and is expressed as

$$n_1(r; U) = \frac{Z_b e \beta_b}{\gamma_b m_b} \frac{A(r)}{\Omega^2 - \omega_\beta^2(r)} n_{0m} \frac{\delta[r - R(U)]}{r} \quad (22)$$

where n_{0m} is the beam density contributed by the energy group labeled by the transverse energy U . Note that $n_b \delta[r - R(U)] = -(d/dr)n_0(r)$. Substituting (22) into (21) and making use of the definition in (6), the perturbed current density of the beam particles are given by

$$J_b(r) = -\frac{Z_b e \beta_b}{\gamma_b m_b} \frac{A(r)}{\Omega^2 - \omega_\beta^2(r)} \frac{1}{r} \frac{d}{dr} J_b^0(r). \quad (23)$$

The eigenvalue equation of the resistive hose instability is obtained by substituting (23) into (17) and is given by

$$\begin{aligned} \frac{d}{dr} \frac{1}{r} \frac{d}{dr} r A(r) + \frac{4\pi i \omega \sigma(r)}{(1 - i\omega/\nu_c) c^2} A(r) \\ = \frac{4\pi Z_b e \beta_b}{\gamma_b m_b c} \frac{A(r)}{\Omega^2 - \omega_\beta^2(r)} \frac{1}{r} \frac{d}{dr} J_b^0(r) \end{aligned} \quad (24)$$

which determine the resistive-hose stability properties of any beam current density profile $J_b^0(r)$, according to the energy

group model of beam dynamics. The treatment of the singularities at $\Omega = \Omega_\beta(r)$ is determined by the requirement that Ω be in the upper half plane. The boundary conditions for the eigenfunction in (22) are $A(r = 0) = A(r = r_w) = 0$, where r_w may be infinite if the beam propagates in a conducting plasma of infinite extent, or where r_w is finite if there is a perfectly conducting guide at $r = r_w$; of course, the case of finite r_w makes sense only if $J_b^0(r = r_w) = 0$. The eigenvalue (24) can be solved numerically for a specified beam-current profile, although we did not attempt to solve it numerically. Instead, approximate solutions of (24), which are valid for long wavelength and low frequency perturbations, will be presented in the subsequent analysis.

III. RESISTIVE-HOSE STABILITY ANALYSIS

The eigenvalue (24) can be solved analytically [28] in the case of the uniform beam current density with a sharp boundary at $r = r_b$, where the right-hand side of (24) is proportional to a delta function, i.e., $\delta(r - r_b)$. Otherwise, the eigenvalues and eigenfunctions of (24) must be calculated numerically. However in this section, we use approximate eigenfunctions to obtain eigenvalues. Multiplying (24) by $rA(r)$ and integrating over r , we obtain the dispersion relation

$$\begin{aligned} \frac{4\pi i \omega}{(1 - i\omega/\nu_c) c^2} \int_0^\infty r dr \sigma(r) A^2(r) \\ = - \int_0^\infty r dr A(r) \frac{d}{dr} \frac{1}{r} \frac{d}{dr} r A(r) \\ + \frac{4\pi Z_b e \beta_b}{\gamma_b m_b c} \int_0^\infty dr \frac{A^2(r)}{\Omega^2 - \omega_\beta^2(r)} \frac{d}{dr} J_b^0(r). \end{aligned} \quad (25)$$

For a given value of the Doppler-shifted frequency Ω , there is generally a discrete set of eigenvalues ω , and eigenfunctions $A(r)$ with different radial mode structures. Our interest here lies in the dipole-mode eigenfunction, which corresponds to a sideways displacement of the beam with a minimum of internal distortion. In the low-frequency limit characterized by

$$4\pi r_b^2 |\omega \sigma| / c^2 \ll 1 \quad (26)$$

the dipole-mode eigenfunction inside the beam is expressed as [23]

$$A(r) \propto \frac{dA_0}{dr} \quad (27)$$

representing a rigid transverse displacement of the rounded beam as well as a self-generated B_θ field, provided that the outer boundary condition is at $r_w = \infty$. The axial component $A_0(r)$ of the equilibrium vector potential is obtained from (9). The axial component $A(r)$ of the perturbed vector potential in (27) corresponds to a rigid displacement of the equilibrium magnetic field. Therefore, one of the reasonable choices of the eigenfunctions is the rigid displacement of the self magnetic field in the plasma, which is represented by (27) for the infinite background plasma ($r_w \rightarrow \infty$). Substituting $A(r) = (d/dr)A_0(r)$ into (25) and making use of (9) and

(11), the dispersion relation of the resistive hose instability is expressed as

$$\begin{aligned} & \frac{i\omega}{c(1-i\omega/\nu_c)} \int_0^\infty r dr \sigma(r) \left[\frac{d}{dr} A_0(r) \right]^2 \\ &= \int_0^\infty r dr \left[\frac{d}{dr} A_0(r) \right] \left[\frac{d}{dr} J_b^0(r) \right] \\ & \quad \left[1 - f + \frac{\omega_\beta^2(r)}{\Omega^2 - \omega_\beta^2(r)} \right] \end{aligned} \quad (28)$$

where use has been made of the assumption that the plasma return current profile is the same as the beam current profile, i.e., $J_p^0(r) = -f J_b^0(r)$.

We introduce a dimensionless parameter $x = r/r_b$, where r_b is the characteristic beam radius. The beam current density is expressed as $J_b^0(r) = J_{bm} q(x)$, where the function $q(x)$ represents the beam current profile. The plasma conductivity $\sigma(r)$ in (28) can also be expressed as $\sigma(r) = \sigma_m s(x)$, where $s(x)$ also represents the conductivity profile. We also remind the reader that the beam current density J_{bm} at the axis is related to the beam number density n_b at the axis by $J_{bm} = Z_b e \beta_b c n_b$. The derivative $(d/dr)A_0(r)$ of the equilibrium vector potential can be expressed as

$$\frac{d}{dr} A_0(r) = -4\pi Z_b e \beta_b (1-f) n_{bm} r_b \frac{1}{x} \int_0^x x' dx' q(x') \quad (29)$$

from (9). The betatron frequency Ω_β defined in (11) can also be expressed as

$$\omega_\beta^2(r) = \omega_{\beta m}^2 h(x) = \frac{2\pi Z_b^2 n_b e^2 \beta_b^2 (1-f)}{\gamma_b m_b} h(x) \quad (30)$$

where the function $h(x)$ is defined by

$$h(x) = \frac{2}{x^2} \int_0^x x' dx' q(x'). \quad (31)$$

The betatron frequency in (30) represents focusing strength of the self magnetic field produced by the beam current. Obviously, the betatron frequency decreases to zero as the fractional current neutralization f approaches to unity. Remember that the beam current profile $q(x)$ has its maximum at the axis and decreases as the radial coordinate r increases for the rounded beam density. Therefore, the function $h(x)$ decreases as the variable x increases. In this context, the betatron frequency decreases from its maximum at the axis as the radial coordinate increases, and the beam particles far away from the axis has a less betatron frequency, thereby falling away from the main body of the beam.

It is useful in the subsequent analysis to define the dimensionless parameter ξ

$$\xi = - \int_0^\infty dx \left(\frac{dq}{dx} \right) \int_0^x x' dx' q(x') \quad (32)$$

which is a positive value due to $dq/dx < 0$ in general. The magnetic decay time τ_d is defined by

$$\tau_d = \frac{4\pi r_b^2 \sigma_m}{c^2} \int_0^\infty dx s(x) \frac{1}{x} \left[\int_0^x x' dx' q(x') \right]^2 \quad (33)$$

which is proportional to the plasma conductivity σ_m , thereby indicating that the self-magnetic field of the beam in a high-conducting plasma takes a longer time to follow the beam deviation. Making use of (29)–(33), the dispersion relation in (28) can then be expressed as

$$i \frac{\omega \tau_d}{1 - i\omega/\nu_c} = \xi - \frac{g(Z)}{1 - f} \quad (34)$$

where the normalized Doppler-shifted frequency-squared Z is defined by $Z = \Omega^2/\omega_{\beta m}^2$ and the function $g(Z)$ is defined by

$$g(Z) = \int_0^\infty dx \left(\frac{dq}{dx} \right) \int_0^x x' dx' q(x') \frac{h(x')}{Z - h(x')}. \quad (35)$$

The dispersion relation in (34) with (35) is one of the main results in this section and can be used to investigate stability properties of the resistive hose instability for a variety of the beam current profiles.

Several points are noteworthy for the integrals $h(x)$, ξ , and $g(Z)$ defined in (31), (32), and (35), respectively. First, the beam current-density profile $q(x)$ has its maximum value of unity at $x = 0$ and decreases continuously as the variable x increases. The function $q(x)$ decreases smoothly at the axis, thereby ensuring $dq/dx = 0$ at $x = 0$ in general. Second, it can be shown that $h(x) = 1$ at $x = 0$, by making use of $dq/dx = 0$ at $x = 0$. Therefore, the integral function $h(x)$ decreases continuously from unity to zero, as the variable x increases from zero to infinity. The maximum betatron frequency $\Omega_{\beta m}$ occurs at the axis, as shown in (30). Third, the integral ξ in (32) is a positive value due to the property of $dq/dx < 0$ in general. Finally, we remind the reader that the denominator $Z - h(x)$ in the right-hand side of (35) is positive for $Z > 1$. Therefore, the integral function $g(Z)$ for the variable Z larger than unity is negative due to $dq/dx < 0$, i.e., $g_r < 0$ and $g_i = 0$ for $Z > 1$, where g_r and g_i are the real and imaginary values of the function $g(Z)$. The imaginary value g_i of $g(Z)$ for $Z > 1$ is zero because of no singularity in the integral in (35). We also note from (35) that $g_r \rightarrow 0$ as $Z \rightarrow \infty$. However, the integral function $g(Z)$ for $Z < 1$ can be any complex value, depending on the current profile $q(x)$ and variable Z .

As an example of the dispersion relation in (34), we consider a uniform density of the beam with a sharp boundary at $r = r_b$. We also assume that the plasma conductivity profile is also the same as the beam current profile. Then, the functions q and s are expressed as

$$q(x) = s(x) = \begin{cases} 1, & x < 1 \\ 0, & x > 1. \end{cases} \quad (36)$$

Substituting (36) into (32), (33), and (35), we can show that $\xi = 1/2$ and $g(Z) = 1/2(Z - 1)$, and that the dispersion

relation in (34) for the flattop density profile is therefore given by

$$\frac{2i\omega\tau_d}{1 - i\omega/\nu_c} - 1 = \frac{1}{(Z - 1)(1 - f)} \quad (37)$$

where the magnetic decay time τ_d is calculated to be $\tau_d = \pi\sigma_m r_b^2/4c^2$ from (33). Equation (37) is identical to the result in a previous literature [28] for $r_w \rightarrow \infty$. We recommend the reader to review the previous literature [28] for detailed stability properties obtained from the dispersion relation in (37).

A finite-size beam pulse is often required to propagate to a target in practical applications. Although the beam head may be at the target, the tail of the beam pulse may deviate from the proposed path due to perturbations that are initiated at the beam head and propagate through the beam pulse, growing during the propagation. In (12), the coordinate τ defined by

$$\tau = t - \frac{z}{\beta_b c} \quad (38)$$

represents the distance (in units of $\beta_b c$) from the beam head to position z . Assuming that each beam segment is taken to oscillate at a fixed real frequency Ω , the frequency Ω represents the growth of the wave as one moves backward from the head of the beam. The real frequency Ω may occur through the dynamics of particular beam segments, and thus scales with the natural oscillation frequency of beam particles, namely the betatron frequency Ω_β , while Ω occurs through the magnetic coupling of different beam segments, and thus scales with the magnetic decay time. Therefore, the discussions in the subsequent analysis are concentrated on the case where the resistive-hose stability properties are investigated for a specified Doppler-shifted frequency Ω . We also point out that the theoretical model developed in Section II has been based on the infinite beam along the axial direction, although the perturbations propagate from the head to tail of the beam. The assumption of the infinite beam along the axial direction is needed for an analytical model developed in Section II. Therefore, the theoretical results in this article are valid for the beam segments located considerably away from the head of the beam.

The dispersion relation of the resistive hose instability can equivalently be expressed as

$$i\omega\tau_d = \frac{[\xi(1 - f) - g(Z)]\nu_c\tau_d}{(\nu_c\tau_d + \xi)(1 - f) - g(Z)} \quad (39)$$

after carrying out a straightforward algebraic manipulation of (34). Value of the integral function $g(Z)$ in (39) can be expressed as $g = g_r + ig_i$ in general, depending on the variable Z . All perturbed quantities are assumed to vary according to $\exp[i(\theta - \Omega z/\beta_b c - \Omega\tau)]$, as shown in (12). Therefore, instability occurs when $\Omega_i = \text{Im}\Omega$ is positive. The growth rate Ω_i and real oscillation-frequency Ω_r in general are obtained by substitution of $g = g_r + ig_i$ into (39). They are given by

$$\omega_i\tau_d = \nu_c\tau_d \frac{[(\nu_c\tau_d + \xi)(1 - f) - g_r][g_r - \xi(1 - f)] - g_i^2}{[(\nu_c\tau_d + \xi)(1 - f) - g_r]^2 + g_i^2} \quad (40)$$

and

$$\omega_r\tau_d = -\frac{\nu_c^2\tau_d^2(1 - f)g_i}{[(\nu_c\tau_d + \xi)(1 - f) - g_r]^2 + g_i^2} \quad (41)$$

which can be used to investigate stability properties of the resistive hose instability for a broad range of physical parameters, including the important influence of the electron collision frequency (ν_c) on stability behaviors. We remind the reader that the perturbation grows only for $\Omega_i\tau_d > 0$, leading to instability.

In the limiting case of highly-collisional plasma characterized by $\nu_c\tau_d \rightarrow \infty$, where the electron collision time ($1/\nu_c$) is much shorter than the magnetic decay time (τ_d), the growth rate and oscillation frequency in (40) and (41) are simplified to

$$\omega_i\tau_d = \frac{g_r}{1 - f} - \xi \quad (42)$$

and

$$\omega_r\tau_d = -\frac{g_i}{1 - f}. \quad (43)$$

The perturbations grow only for the range of g_r satisfying $g_r > \xi(1 - f)$. It is obvious from (42) that the growth rate of the resistive hose instability in collisional plasmas characterized by $\nu_c\tau_d \rightarrow \infty$ increases drastically as the fractional current neutralization f approaches unity. Preliminary experiment [20] has been carried out for $\nu_c\tau_d \rightarrow \infty$ and $f = 0$.

As a second example, we consider the case of $g_i = 0$, where the real oscillation frequency Ω_r is zero, indicating a pure growth, and the necessary and sufficient condition of instability is given by

$$\xi(1 - f) < g_r < (\nu_c\tau_d + \xi)(1 - f) \quad (44)$$

from (40). We note from (44) that the width of the range of the integral function g corresponding to instability for $g_i = 0$ is given by

$$\Delta g = \nu_c\tau_d(1 - f) \quad (45)$$

which decreases drastically as value of the parameter $\nu_c\tau_d$ decreases from infinity to zero or the fractional current neutralization f approaches unity. Note from (35) that the integral g is a function of the normalized frequency-squared Z . Therefore, the width of the range Z corresponding to instability may also be restricted by values of the parameter $\nu_c\tau_d$ and of the fractional current neutralization f . In this context, we may show that the width of the range Ω^2 corresponding to instability is given by

$$\begin{aligned} \Delta\Omega^2 &= \frac{2\pi Z_b^2 n_b e^2 \beta_b^2 (1 - f)}{\gamma_b m_b} \Delta Z \\ &= (1 - f)W[\nu_c\tau_d, (1 - f)] \end{aligned} \quad (46)$$

where the function W is an increasing function of parameter $\nu_c\tau_d$ and $1 - f$. In obtaining (46), use has been made of $Z = \Omega^2/\Omega_{\beta m}^2$ and of the definition of $\Omega_{\beta m}^2$ in (30). We, therefore, conclude from (46) that the width of the range Ω^2 corresponding to instability decreases drastically as the value of the parameter $\nu_c\tau_d$ decreases from infinity to zero and the fractional current neutralization f approaches unity, thereby being a very narrow bandwidth of instability. Thus, the instability caused by the dynamics of the particle beam segments with frequency Ω may easily be avoided by choosing proper system parameters for a

finite value of the parameter $\nu_c\tau_d$. However, the growth rate increases drastically as the fractional current neutralization f approaches unity, as shown in (42). The instability condition in (44) for $g_i = 0$ can also be expressed as

$$\frac{g_r}{\nu_c\tau_d + \xi} < 1 - f < \frac{g_r}{\xi} \quad (47)$$

which indicates that the range of the fractional current neutralization f corresponding to instability reduces drastically as the parameter $\nu_c\tau_d$ decreases from infinity to zero. According to (42), the larger the integral function g_r is the higher the growth rate for $\nu_c\tau_d \gg 1$. On the other hand, the left-hand side of (47) can easily be larger than unity for parameter $\nu_c\tau_d$ comparable to or less than ξ , thereby stabilizing the system.

The integral function $g(Z)$ has a negative value for $Z > 1$, as mentioned earlier, showing $g_r < 0$ and $g_i = 0$ for $Z > 1$. A negative value of g_r never satisfies the inequality in (44), ensuring stability. Any perturbation with the normalized frequency-squared Z higher than unity is purely damping. Note from the definition of $Z = \Omega^2/\Omega_{\beta m}^2$ that the Doppler-shifted frequency Ω seen by beam particles for $Z > 1$ is higher than the maximum betatron frequency $\Omega_{\beta m}$. There is no beam particle for $Z > 1$, which is in resonance with the frequency Ω of perturbations. Therefore, the perturbations for $Z > 1$ are purely damping for $\Omega^2 > \Omega_{\beta m}^2$ for arbitrary current profile.

In the extreme limit where the electron collision time ($1/\nu_c$) is far longer than the magnetic decay time (τ_d) characterized by the parameter $\nu_c\tau_d$ much less than ξ , i.e., $\nu_c\tau_d \ll \xi$, the growth rate $\Omega_i\tau_d$ and real oscillation frequency $\Omega_r\tau_d$ in (40) and (41) are simplified to

$$\omega_i\tau_d = -\nu_c\tau_d \quad (48)$$

and

$$\omega_r\tau = -(\nu_c\tau_d)^2 \frac{(1-f)g_i}{[\xi(1-f) - g_r]^2 + g_i^2}. \quad (49)$$

The growth rate in (48) is a negative value, ensuring stability for the resistive hose perturbations. Note from (49) that the real oscillation frequency is proportional to the square of a small value of parameter $\nu_c\tau_d$, thereby indicating that any perturbation is almost purely damping for $\nu_c\tau_d \rightarrow 0$.

IV. RESISTIVE-HOSE STABILITY PROPERTIES OF A BEAM WITH BENNETT CURRENT PROFILE

One of the most common profiles of the charged particle-beam current is the Bennett profile given by [34]

$$q(x) = \frac{1}{(1+x^2)^2}. \quad (50)$$

Substituting (50) into (31) gives

$$h(x) = \sqrt{q(x)} = \frac{1}{1+x^2} \quad (51)$$

which is useful in the subsequent analysis. Note that $h(0) = 1$ and $h(\infty) = 0$. Substituting (50) into (32) and changing the integral variable from x to h , we obtain $\xi = 1/6$ after a straight-

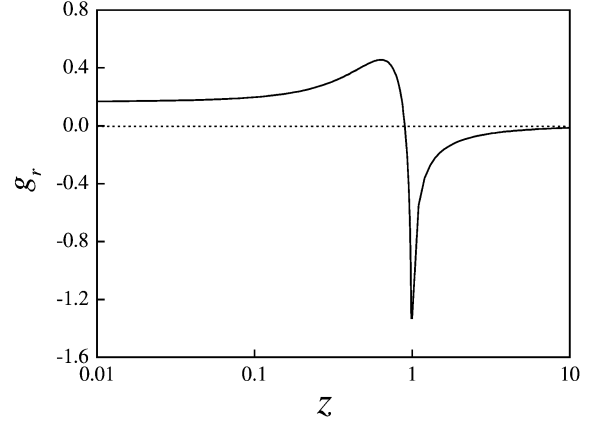


Fig. 1. Plot of the real value g_r of the integral $g(Z)$ versus the normalized Doppler-shifted frequency-squared Z for Bennett current profile.

forward calculation. The integral function $g(Z) = g_r + ig_i$ is calculated by substituting (50) and (51) into (35) and by making use of the integral variable h instead of x . After carrying out a tedious but straightforward algebraic manipulation, we obtain

$$g_r = \left(\frac{1}{6} + \frac{Z}{4} + \frac{Z^2}{2} - \frac{Z^3}{2} \ln \left| \frac{Z}{Z-1} \right| \right) \quad (52)$$

and

$$g_i = \begin{cases} Z^3\pi/2, & Z < 1 \\ 0, & Z > 1. \end{cases} \quad (53)$$

Shown in Fig. 1 is plot of the real value g_r of the integral $g(Z)$ versus the normalized Doppler-shifted frequency-squared Z for Bennett current profile. The real value g_r increases from $1/6$, peaks and then decreases drastically, as the frequency-squared Z approaches from zero to unity. The imaginary value g_i of the integral $g(Z)$ increases continuously from zero to $\pi/2$, as the frequency-squared Z approaches from zero to unity. As discussed in Section III, the real value g_r is negative and the imaginary value g_i is zero for the variable Z beyond unity, thereby not satisfying (44) for arbitrary values of parameter $\nu_c\tau_d$ and the current neutralization f . We therefore conclude that the charged particle beams are stable for the resistive hose instability with the beam segment perturbations of the frequency-squared Z beyond unity. The real value g_r in (52) is approximated by $g_r = -1/12Z$ for $Z \gg 1$, thereby approaching zero as Z increases to infinity.

To complete the analysis, we substitute (51) into (33) and obtain

$$\tau_d = \frac{\pi r_b^2 \sigma_m}{2c^2} \int_0^1 dh (h^{-1} - 1)s(h). \quad (54)$$

Assuming that the plasma conductivity profile $s(x)$ is the same as the beam current profile, i.e., $q(x) = s(x)$ in (50), the magnetic decay time in (54) is calculated to be

$$\tau_d = \frac{\pi r_b^2 \sigma_m}{12c^2} \quad (55)$$

which can be used for evaluation of the magnetic decay time.

As an illustrative example, which is characteristic of heavy ion fusion applications [27], we consider a 1 kA cesium ion beam corresponding to mass number $A = m_b/m_p = 137$. The

beam ions are singly charged with $Z_b = 1$, and the average kinetic energy is $(\gamma_b - 1)m_b c^2 = 2.5$ GeV corresponding to $\beta_b = 0.2$. Assuming that the beam radius is $r_b = 1$ cm, the beam density is calculated to be $n_b = 10^{12}$ cm $^{-3}$. The corresponding betatron frequency at the axis calculated from (30) is $\Omega_{\beta m} = 1.5 \times 10^7$ s $^{-1}$, assuming zero return current ($f = 0$). The electron collision frequency for Coulomb collisions is given by [35]

$$\nu_c = 2.9 \times 10^{-6} n_e \ln \Lambda T_e^{-3/2} \quad (56)$$

where the typical value of the Coulomb logarithm is about $\ln \Lambda = 10$. Assuming the electron temperature is about $T_e = 1$ eV and taking $n_e = 5 \times 10^{12}$ cm $^{-3}$, the electron collision frequency is $\nu_c = 1.5 \times 10^8$ s $^{-1}$, which is considerably higher than the betatron frequency. The conductivity of the background plasma (assumed fully ionized) can be expressed as [36]

$$\sigma = \frac{3m_e}{(16/\sqrt{\pi})Ze^2 \ln \Lambda} \left(\frac{2\kappa T_e}{m_e} \right)^{3/2} \quad (57)$$

where κ is Boltzmann's constant. From (57), for $T_e = 1$ eV and $\ln \Lambda = 10$, the conductivity is $\sigma_m = 3 \times 10^{12}$ s $^{-1}$. Therefore, the magnetic decay time defined in (55) is calculated to be $\tau_d = 9 \times 10^{-10}$ s. Value of the parameter $\nu_c \tau_d$ in this particular example is given by $\nu_c \tau_d = 0.135$, which is much less than unity.

Stability properties of the resistive hose instability in a charged particle beam with Bennett current profile can be investigated for the variable Z in the range of $Z < 1$ by substituting (52) and (53) into (40) and (41). Fig. 2 presents plots of (a) the normalized growth rate $\Omega_i \tau_d$ and (b) the real oscillation frequency $\Omega_r \tau_d$ versus the normalized Doppler-shifted frequency-squared Z obtained from (40), (41), (52), and (53) for Bennett current profile, $f = 0$, and $\nu_c \tau_d = 0.1$ and ∞ . As expected from (44) and Fig. 1, the normalized growth rate $\Omega_i \tau_d$ is calculated to be negative in the range of Z satisfying $Z > 1$, where the resistive hose perturbations in the Bennett profile beam are stable. The real oscillation frequency $\Omega_r \tau_d$ is calculated to be negative throughout the presentation in this section due to the positive value of g_i in (53). Shown in Fig. 3 are plots of (a) the normalized growth rate $\Omega_i \tau_d$ and (b) the real oscillation frequency $\Omega_r \tau_d$ versus the normalized Doppler-shifted frequency-squared Z obtained from (40), (41), (52), and (53) for Bennett current profile, $f = 0.2$, and $\nu_c \tau_d = 0.1$ and ∞ . As expected from the discussions in Section III, we note from Fig. 3 that the width of the range Z corresponding to instability is very narrow for a small value of $\nu_c \tau_d = 0.1$. Note that the horizontal line in Figs. 2 and 3 is in the log scale. The unstable range of variable Z in Fig. 3 for $\nu_c \tau_d = 0.1$ is about one tenth of that for $\nu_c \tau_d = \infty$. Instability occurs in a very narrow range of the variable Z for a small value of $\nu_c \tau_d$ in general. Therefore, we may easily avoid this unstable range of the frequency-squared Z by carefully choosing the system parameters. Comparing Figs. 2 and 3, we note that the growth rate increases considerably even for a moderate increase of the fractional current neutralization.

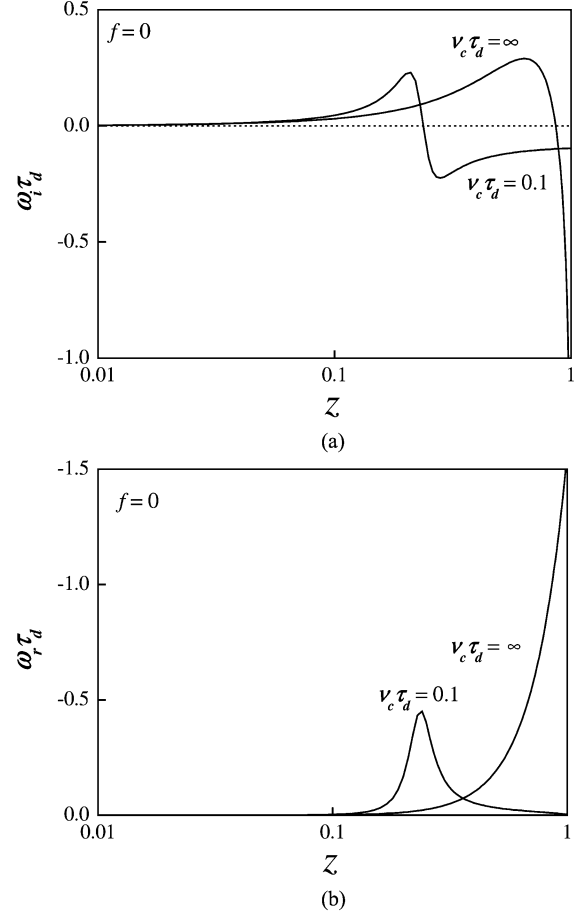


Fig. 2. Plots of (a) the normalized growth rate $\Omega_i \tau_d$ and (b) the real oscillation frequency $\Omega_r \tau_d$ versus the normalized Doppler-shifted frequency-squared Z obtained from (40), (41), (52), and (53) for Bennett current profile, $f = 0$, and $\nu_c \tau_d = 0.1$ and ∞ .

Presented in Fig. 4 are plots of (a) the normalized growth rate $\Omega_i \tau_d$ and (b) the real oscillation frequency $\Omega_r \tau_d$ versus the parameter $\nu_c \tau_d$ obtained from (40), (41), (52), and (53) for Bennett current profile, $Z = 0.64$ corresponding to $g_r = 0.456$ and $g_i = 0.392$, and $f = 0$ and 0.2 . Note $\xi = 0.166$. As expected from the left-hand side of (47), Fig. 4 indicates that a small value of parameter $\nu_c \tau_d$ has a strong stabilizing influence on the resistive hose perturbations. The damping rate (a negative value of $\Omega_i \tau_d$) in Fig. 4 is scaled to $\nu_c \tau_d$ for $\nu_c \tau_d \ll 1$, as predicted from (48).

V. CONCLUSION

Stability properties of the resistive hose instability were investigated in this article for a rounded current-density profile of a charged particle beam propagating through a background plasma where the electron collision time ($1/\nu_c$) is comparable to the magnetic decay time (τ_d). The basic assumptions and theoretical model were presented in Section II for an intense charged particle beam with a rounded density profile. The eigenvalue equation was derived based on the energy group model, assuming long-wavelength, low-frequency perturbations and the complete charge neutralization of the perturbed beam space-charge field. The eigenvalue equation obtained in Section II includes the stabilizing influence of a finite magnetic

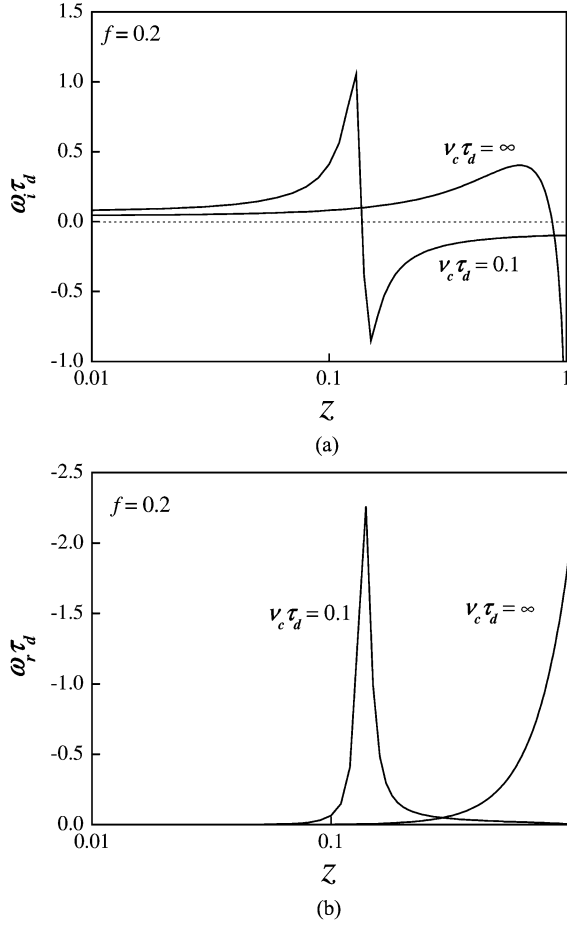


Fig. 3. Plots of (a) the normalized growth rate $\Omega_i \tau_d$ and the real oscillation frequency $\Omega_r \tau_d$ versus the normalized Doppler-shifted frequency-squared Z obtained from (40), (41), (52), and (53) for Bennett current profile, $f = 0.2$, and $\nu_c \tau_d = 0.1$ and ∞ .

decay time, which can be comparable to or shorter than the electron collision time ($1/\nu_c$).

The dispersion relation of the resistive hose instability in a charged particle beam with an arbitrary current density profile was derived in Section III, assuming that the eigenfunctions can be represented by the rigid displacement of the self magnetic field in the plasma. Stability analysis for perturbations propagating through the beam pulse from its head to tail was carried out in Section III for an arbitrary current profile of the beam, by selecting z and τ as independent variables. The complex eigenfrequency ω in the dispersion relation of the resistive hose instability in a beam with an arbitrary current profile was expressed as a function of the real oscillation frequency Ω of each beam segment. It was shown from the stability analysis in Section III that the width of the range Ω^2 corresponding to instability decreases drastically as the value of the parameter $\nu_c \tau_d$ decreases from infinity to zero and the fractional current neutralization f approaches unity, thereby being a very narrow bandwidth of instability. Thus, the instability caused by the dynamics of the beam segments with frequency Ω may easily be avoided by choosing proper system parameters for a finite value of the parameter $\nu_c \tau_d$, which can be much less than unity in some practical applications. It was also shown for arbitrary current profile that any perturbation with frequency Ω higher than the max-

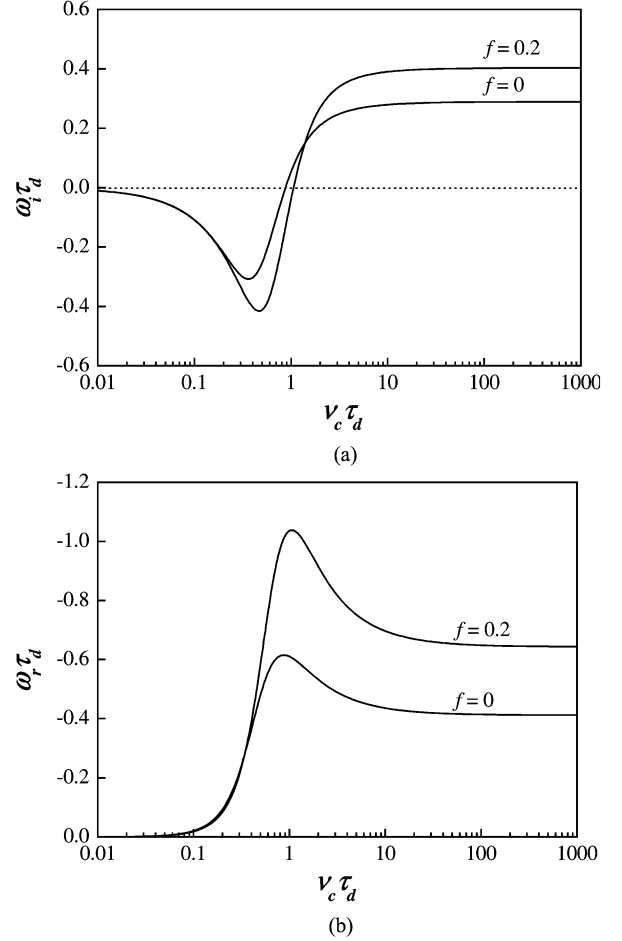


Fig. 4. Plots of (a) the normalized growth rate $\Omega_i \tau_d$ and (b) the real oscillation frequency $\Omega_r \tau_d$ versus the parameter $\nu_c \tau_d$ obtained from (40), (41), (52), and (53) for Bennett current profile, $Z = 0.64$ corresponding to $g_r = 0.114$ and $g_i = 0.098$, and $f = 0$ and 0.2 .

imum betatron frequency $\Omega_{\beta m}$ is stable (purely damping). Stability properties of the resistive hose instability in a beam with Bennett current profile were investigated in Section IV as an example of the rounded beam density. Stability properties analyzed numerically in Section IV for the Bennett current profile agree well with the general discussions in Section III for an arbitrary current profile.

Finally, we conclude this article pointing out that the stability analysis has been carried out for a self-pinch particle beam, whose density is a monotonously decreasing function of the radial coordinate. However, the density of the charged particle beam can also be hollow, if there is any external force like an external applied magnetic field or a plasma return current at the axis. In this case, the betatron frequency $\Omega_{\beta}(r)$ defined in (11) must be considerably modified and the stability analysis may lead to the multi-resonance layer problem. The resistive-hose instability in a hollow charged-particle beam is current under investigation by us, hoping that the useful results will be published elsewhere.

REFERENCES

- [1] R. C. Davidson, *Physics of Nonneutral Plasmas*. Reading, MA: Addison-Wesley, 1990.

- [2] A. W. Chao, *Physics of Collective Beam Instabilities in High Energy Accelerators*. New York: Wiley, 1993.
- [3] M. Reiser, *Theory and Design of Charged Particle Beams*. New York: Wiley, 1994.
- [4] J. D. Lawson, *The Physics of Charged-Particle Beams*. New York: Oxford Science, 1988.
- [5] R. C. Davidson and H. Qin, *Physics of Intense Charged Particle Beam in High Energy Accelerator*, Singapore: World Scientific, 2001.
- [6] R. A. Jameson, *Advanced Accelerator Concepts, American Institute of Physics Conference Proceedings*, J. S. Wurtele, Ed. New York: Amer. Inst. Phys., 1993, vol. 279, p. 969.
- [7] E. P. Lee and J. Hovington, *Fusion Technology*, 1989, vol. 15, p. 369.
- [8] "Physics design and scaling of recirculating induction accelerators: From benchtop prototypes to drivers," in *Proc. 1995 Int. Symp. Heavy Ion Inertial Fusion*, vol. 32, J. J. Barnard, T. J. Fessenden, and E. P. Lee, Eds., 1996, pp. 1–620.
- [9] D. G. Koshkarev and P. R. Zenkevich, "Ion resonance instability in an electron ring accelerator," *Particle Accelerators*, vol. 3, p. 1, 1972.
- [10] R. C. Davidson and H. S. Uhm, "Coupled dipole oscillation of intense relativistic electron beam," *J. Appl. Phys.*, vol. 51, p. 885, 1980.
- [11] —, "Influence of finite ion larmor radius effects on the ion resonance instability in a nonneutral plasma column," *Phys. Fluids*, vol. 21, p. 60, 1978.
- [12] D. Neuffer, E. Colton, D. Fitzgerald, T. Hardek, R. Hutson, R. Macek, M. Plum, H. Thiessen, and T. S. Wang, "Observations of a fast transverse instability in the PSR," *Nucl. Instrum. Methods Phys. Res.*, vol. A321, p. 1, 1992.
- [13] D. Neuffer and C. Ohmori, "Calculations of the conditions for bunch leakage in the Los Alamos proton storage ring," *Nucl. Instrum. Methods Phys. Res.*, vol. A343, p. 390, 1994.
- [14] M. Izawa, Y. Sato, and T. Toyomasu, "The vertical instability in a positron bunched beam," *Phys. Rev. Lett.*, vol. 74, p. 5044, 1995.
- [15] J. Byrd, A. Chao, S. Heifets, M. Minty, T. O. Roubenheimer, J. Seeman, G. Stupakov, J. Thomson, and F. Zimmerman, "First observations of a fast beam-ion instability," *Phys. Rev. Lett.*, vol. 79, 1997.
- [16] E. Keil and B. Zotter, CERN Rep. CERN_ISR-TH/71-58, 1971.
- [17] R. C. Davidson, H. Qin, P. H. Stoltz, and T. S. Wang, "Kinetic description of electron-proton instability in high-intensity proton linacs and storage rings based on the Vlasov-Maxwell equations," *Phys. Rev. Special Topics Accel. Beams*, vol. 2, p. 054 401, 1999.
- [18] R. C. Davidson and H. S. Uhm, "Effects of the solenoid focusing field on the electron-ion two-stream instability in high intensity ion beams," *Physics Lett.*, vol. A 285, p. 88, 2001.
- [19] H. S. Uhm, R. C. Davidson, and I. Kaganovich, "Two-stream sausage and hollowing instabilities in high-intensity particle beams," *Phys. Plasmas*, vol. 8, p. 4637, 2001.
- [20] E. J. Lauer, R. J. Briggs, T. J. Fessenden, R. E. Hester, and E. P. Lee, "Measurements of hose instability of a relativistic electron beam," *Phys. Fluids*, vol. 21, p. 1344, 1978.
- [21] M. N. Rosenbluth, "Long-wavelength beam instability," *Phys. Fluids*, vol. 3, p. 932, 1960.
- [22] E. P. Lee, "Resistive hose instability of a beam with the bennett profile," *Phys. Fluids*, vol. 21, p. 1327, 1978.
- [23] H. S. Uhm and M. Lampe, "Theory of the resistive hose instability in relativistic electron beams," *Phys. Fluids*, vol. 23, p. 1574, 1980.
- [24] —, "Stability properties of azimuthally symmetric perturbations in an intense electron beam," *Phys. Fluids*, vol. 24, p. 1553, 1981.
- [25] G. Joyce and M. Lampe, "Numerical simulation of the axisymmetric hollowing instability of a propagating beam," *Phys. Fluids*, vol. 26, p. 3377, 1983.
- [26] H. S. Uhm, "An abbreviated instructive description of the resistive hose instability," *Amer. J. Phys.*, vol. 48, p. 270, 1980.
- [27] H. S. Uhm and R. C. Davidson, "Effects of the plasma conductivity on transverse instabilities in high-intensity ion beam," *IEEE Trans. Plasma Sci.*, vol. 32, no. 2, pp. 440–447, Apr. 2004.
- [28] —, "Effects of the electron collisions on the resistive instability in intense charged particle beams propagating through a background plasmas," *Phys. Rev. Special Topics Accel. Beams*, vol. 6, p. 034 204, 2003.
- [29] C. L. Olson, "Chamber transport [heavy ion fusion]," *Nucl. Instrum. Methods Phys. Res.*, vol. 464, p. 118, 2002.
- [30] D. V. Rose, P. F. Ottinger, D. R. Welch, B. V. Oliver, and C. L. Olson, "Numerical simulations of self-pinch transport of intense ion beams in low-pressure gases," *Phys. Plasmas*, vol. 6, p. 4094, 1999.
- [31] D. R. Welch, D. V. Rose, B. V. Oliver, T. C. Genoni, C. L. Olson, and S. S. Yu, "Simulations of intense heavy ion beams propagating through a gaseous fusion target chamber," *Phys. Plasmas*, vol. 9, p. 2344, 2002.
- [32] R. C. Davidson *et al.*, "Overview of theory and modeling in the heavy ion fusion virtual national laboratory," *Laser Part. Beams*, vol. 20, p. 377, 2002.
- [33] I. D. Kaganovich, G. Shevet, E. Startsev, and R. C. Davidson, "Nonlinear charge and current neutralization of an ion beam pulse in a pre-formed plasma," *Phys. Plasmas*, vol. 8, p. 4180, 2001.
- [34] W. H. Bennett, "Magnetically self-pinch streams," *Phys. Rev.*, vol. 45, p. 890, 1934.
- [35] H. L. Anderson, Ed., *Physicist's Desk Reference*. New York: Amer. Inst. Phys., 1989, ch. 18.
- [36] N. A. Krall and A. W. Trivelpiece, *Principles of Plasma Physics*. New York: McGraw-Hill, 1973, ch. 6.



Han S. Uhm (A'84–M'87–SM'87) received the Ph.D. degree from University of Maryland, College Park, in 1976.

He was with the Naval Surface Warfare Center from 1978 to 1999. He is professor at Ajou University, Suwon, Korea. The major research areas where he is recognized as a technical expert are as follows: charged particle beams (charged particle-beam propagation in air, beam properties in particle accelerators, collective ion acceleration and high-power electrical pulse system); high-power microwave

generations (gyrotron, magnetron, free electron laser and klystron); plasma material processing (large-volume plasma generations for plasma processing, focused ion-beam generation, and plasma ion implantation for wear and corrosion resistance materials); neutron transport physics (neutron radiography and shallow-water mine detection); plasma chemistry (plasma-assisted chemical vapor elimination and air purification); the atmospheric plasma generations and applications.



Ronald C. Davidson received the B.Sc. degree from McMaster University, Hamilton, ON, Canada, in 1963, and the Ph.D. degree from Princeton University, Princeton, NJ, in 1966.

He has been Professor of Astrophysical Sciences at Princeton University since 1991, and was Director of the Princeton Plasma Physics Laboratory from 1991 to 1996. He was Assistant Research Physicist at the University of California, Berkeley, from 1966 to 1968, an Assistant Professor of Physics at the University of Maryland, College Park, from 1968 to 1971, an Alfred P. Sloan Foundation Fellow from 1970 to 1972, an Associate Professor of Physics from 1971 to 1973, a Professor of Physics at the University of Maryland from 1973 to 1978, and Professor of Physics at the Massachusetts Institute of Technology (MIT), Cambridge, from 1978 to 1991. He has made numerous fundamental theoretical contributions to several areas of pure and applied plasma physics, including nonneutral plasmas, nonlinear effects and anomalous transport, kinetic equilibrium and stability properties, intense charged particle beam propagation in high energy accelerators, and coherent radiation generation by relativistic electrons. He is the author of more than 300 journal articles and books, including four advanced research monographs: *Methods in Nonlinear Plasma Theory* (New York: Academic Press, 1972), *Theory of Nonneutral Plasmas* (New York: W.A. Benjamin, 1974), *Physics of Nonneutral Plasmas* (New York: Addison-Wesley, 1990), and *Physics of Intense Charged Particle Beams in High Energy Accelerators*, with Hong Qin (Singapore: World Scientific, 2001). During 1976–1978, he served as Assistant Director for Applied Plasma Physics, Office of Fusion Energy, Department of Energy. He also served as Director of the MIT Plasma Fusion Center from 1978 to 1988, as the first Chairman of the DOE Magnetic Fusion Advisory Committee (MFAC) from 1982 to 1986, as Chair of the American Physical Society's Division of Plasma Physics during 1983–1984 and Division of Physics of Beams during 2001–2002, and has participated in numerous national and international committees on plasma physics and fusion research.

Dr. Davidson is a Fellow of the American Physical Society, a Fellow of the American Association for the Advancement of Science, and a Member of Sigma Xi. He is also a recipient of the Department of Energy's Distinguished Associate Award and the Fusion Power Associates Leadership Award, both in 1986, and recipient of The Kaul Foundation's Award for Excellence in Plasma Physics Research in 1993.